PAPER • **OPEN ACCESS**

The possible role of the vagal nervous system in the recovery of the blood pressure control after cardiac arrest: a porcine model study

To cite this article: Mario Lavanga *et al* 2017 *Physiol. Meas.* **38** 63

OPEN ACCESS
IOP Publishing | Institute of Physics and Engineering in Medicine Physiological Measurement
Physiol. Meas. **38** (2017) 63–76 doi:10.1088/1361-6579/38/1/63

The possible role of the vagal nervous system in the recovery of the blood pressure control after cardiac arrest: a porcine model study

Mario Lavanga[1,2], Giuseppe Baselli[1], Francesca Fumagalli[3], Giuseppe Ristagno[3] and Manuela Ferrario[1]

[1] Department of Electronics, Information and Bioengineering, Politecnico di Milano, P.zza Leonardo da Vinci 32, Milan, Italy
[2] ESAT—STADIUS, KU Leuven, Kasteelpark Arenberg 10, box 2446, 3001 Leuven, Belgium
[3] IRCCS Istituto di Ricerche Farmacologiche Mario Negri, Via La Masa, 19, 20156 Milano, Italy

E-mail: manuela.ferrario@polimi.it

Received 3 May 2016, revised 12 October 2016
Accepted for publication 19 October 2016
Published 12 December 2016

Abstract

Previous studies have proved that the baroreceptor reflex (baroreflex) control of heart rate can be used for stratification of post-infarction population and, in general, cardiovascular disease populations. Many methods have been proposed to estimate the so-called baroreflex sensitivity (BRS) expressed as ms $mmhg^{-1}$. Most of the studies that exploit BRS focus mainly on acute myocardial infarction (AMI) and there are no important works that investigate the role of BRS immediately after cardiac arrest (CA). The present work is a continuation of the published work of Ristagno *et al* (2014 *Shock* **41** 72–8). In particular, the main objectives are: (1) to study the evolution of BRS after CA and following cardiopulmonary resuscitation (CPR); (2) to verify if the recovery of cardiovascular stability and arterial blood pressure is accompanied by a recovery of BR in a porcine model; (3) to investigate the possible causes of the BRS variations in response to CA and following cardiopulmonary resuscitation. All the BRS estimators adopted in this study show a significant decrease after CA. However, partial recovery is obtained in the last hours of post resuscitation. Analysis of impulse response showed a decrease in peak delay after CA and was significantly shorter 4 hours after CPR. This finding

hints at a compensation mechanism: a faster response when baroreflex gain is not fully restored. The increase in the speed of baroreflex response is in line with the hypothesis of a key role of the parasympathetic nervous system, which is known to act at a higher firing rate.

Keywords: baroreflex sensitivity, autonomic nervous system, CA, bivariate model, impulse response, vagal activity

(Some figures may appear in colour only in the online journal)

1. Introduction

The role of the autonomic nervous system in maintaining blood pressure and its regulation is decisive. Several studies proved that the baroreceptor reflex (baroreflex) control of heart rate can be used for stratification of post-infarction population and, in general, cardiovascular disease populations (La Rovere *et al* 2011). The baroreflex can be assessed using different methods either invasively, by means of pharmacological maneuvers, or non-invasively, i.e. in spontaneous conditions. Those methods provide the baroreflex estimate known as baroreflex sensitivity (BRS) expressed as ms mmhg^{-1} (Baselli *et al* 1988, Barbieri *et al* 2001, Porta *et al* 2006, Aletti *et al* 2012).

In addition, most studies on BRS are focused on acute myocardial infarction and there are no important studies that investigate the role of BRS immediately after CA. According to the American Heart Association, CA is caused by heart electrical system malfunctions such as ventricular fibrillation, or it can be consequent to myocardial ischemia due to coronary occlusion.A common counter-measure to reverse this life-threatening event is cardiopulmonary resuscitation (CPR) in order to restore reperfusion and defibrillation to restore the normal heart rhythm. Gräsner and Bossaert (2013) reported that the average incidence of the out-of-hospital CA (OHCA) is 38.7/100 000 per year in Europe in a study that involved 37 communities. They also found average OHCA incidence equal to 55/100 000 per year in the USA (considering the data represented in the study period 1980–2003).

Post-resuscitation myocardial dysfunction, including arterial hypotension, ventricular arrhythmias, and recurrent CA, along with uncoupling of the autonomic nervous system (ANS) and cardiovascular system, has been recognized as a leading cause of early death after initially successful resuscitation. Approximately 70% of successfully resuscitated victims of CA die within the first 72 h, mainly due to severe myocardial dysfunction (Nolan *et al* 2008). In approximately two thirds of CA events, the usual cause is underlying acute ischemic heart disease (Podrid and Myerburg 2005). The ischemia-induced ventricular fibrillation model is associated with increases in the defibrillation threshold and with more frequent premature ventricular beats and recurrence of ventricular fibrillation. The experimental model proposed in the present work, i.e. a partial LAD occlusion induced myocardial ischemia plus malignant arrhythmia, accounted for the less favorable outcomes and for the severity of post-resuscitation myocardial dysfunction (Ristagno *et al* 2007). Thus, in this study we offer a more clinically relevant experimental model.

The change of baroreceptor reflex was proved to be able to stratify patients after myocardial infarction in a similar way to a commonly used reperfusion marker, i.e. ST-resolution (De Ferrari *et al* 2014). In this particular work (De Ferrari *et al* 2014), the authors hypothesized that the reduction of baroreflex gain is caused by an increase in afferent discharge associated to the left ventricle's altered geometry, caused in turn by myocardial ischemia and necrosis. The authors assessed the BRS among myocardial infarction patients after primary percutaneous

coronary intervention within the first 12 h from intervention. They interpreted their results with an increase in sympathetic activity to be as a consequence, as well as a decrease of a vagal stimulation. Finally, they suggested the protective role of the vagus nerve from arrhythmias, also highlighting its ability to limit the inflammatory response and infarct size.

Baroreflex is the direct expression of nervous regulation of the heart rate and arterial blood pressure (ABP) and can provide an overall assessment of altered conditions in the ANS and the cardiovascular system at the same time. Nevertheless, to the best of our knowledge no studies have been performed that focus on the evolution of baroreflex control after CA or use it as a predictive marker on the clinical progress or outcome. How the baroreflex changes after CA could provide further knowledge about regulatory mechanisms of the cardiovascular system altered by this condition. The evidence of a key role of the parasympathetic nervous system could pave the way for more targeted treatment.

The current work is a continuation of the published work of Ristagno *et al* (2014), where the neuroprotective role of argon was investigated in 12 pigs after CA. In particular, argon was used as substitute for nitrogen during mechanical ventilation. The experimental setup and animal data have been described earlier (Ristagno *et al* 2014). The purpose of this study is to investigate the ANS and blood pressure control in an experimental study of CA in a porcine model. In particular, the specific purposes of this study were: (i) to study the changes and potential recovery of baroreflex within the first 4 h after CPR, in a similar way as described above (De Ferrari *et al* 2014); (ii) to verify if the recovery of cardiovascular stability and arterial blood pressure is accompanied or driven by a recovery in BRS values; (iii) to investigate the possible factors which drive the baroreflex response to CA and following cardiopulmonary resuscitation. Finally, a comparison between the two treatments was performed for completeness.

To reach these objectives, different mathematical methods were examined, such as the impulse response analysis so to investigate the dynamic response of baroreflex and not only the absolute gain.

2. Materials and methods

2.1. Experimental protocol and data

The details of the study are illustrated in a previous work (Ristagno *et al* 2014). Briefly, 12 male pigs (38 ± 1 kg) received anesthesia by intramuscular injection of ketamine (20 mg kg^{-1}) and completed by ear vein injection of sodium pentobarbital (30 mg kg^{-1}). Animals were mechanically ventilated with a tidal volume of 15 ml kg^{-1} and FiO_2 of 0.2 l. The arterial blood pressure was continuously measured by a fluid-filled 7F catheter placed in the thoracic aorta from the right femoral artery. Myocardial infarction was induced in a closed-chest preparation by intraluminal occlusion of the left anterior descending (LAD) coronary artery (Ristagno *et al* 2014). For inducing ventricular fibrillation, a 5F pacing catheter was advanced from the right subclavian vein into the right ventricle. After the CA, CPR was performed. Successful resuscitation was defined as restoration of an organized cardiac rhythm with a mean arterial pressure (MAP) higher than 60 mmHg for more than 1 min. After that, if ventricular fibrillation reoccurred, it was treated by immediate defibrillation. After successful resuscitation, anesthesia was maintained, and animals were monitored for the following 4 h.

The animals were allocated into one of two study groups: (a) the argon group consisted of animals ventilated during the resuscitation with a gas mixture composed by 70% argon and 30% oxygen; or (b) a control group consisting of animals ventilated with a standard gas mixture, i.e. a mix of 70% nitrogen and 30% oxygen. Argon or control treatment was initiated

within 5 min following resuscitation, after hemodynamic stabilization and was maintained for 4 h.

Hemodynamics data were recorded continuously (WinDaq, DATAQ Instruments Inc, Akron, OH) at a sampling rate of 100 Hz.

2.2. Data preprocessing

The ABP signals were subdivided into five epochs. The portion of the recording just before the LAD occlusion was selected as the pre-CA phase. We had no a baseline phase before the anesthesia induction due to technical reasons. The other epochs were the post-resuscitation (Pr) phases consisting of segments of about 15 min within the 4 h after the stabilization of the animal and named as Pr 1 h, Pr 2 h, Pr 3 h and Pr 4 h. All the clinical events, the occlusion as well as the CPR, were annotated by the medical surgeon as a time marker in the signal files. For each phase, a window of ABP with a length ranging from 10 to 15 min was extracted by eyeballing. The windows were chosen to maximize the percentage of good quality heart cycles and were stationary. Each window was further divided into 50% overlapping 3 min segments.

All the analyses were performed in a MATLAB® environment. For each segment we applied an automatic algorithm for the identification of the onset of heart cycle on the ABP waveform (Zong *et al* 2003). The systolic arterial pressure (SAP) and diastolic arterial pressure (DAP) were identified respectively as the local maximum and minimum in time interval following the onset. The pulse pressure (PP) was estimated as the difference between the SAP value of the current cardiac cycle and the DAP value of the previous one. The heart cycle duration was estimated by considering the heart period (HP), which is the difference of two consecutive ABP onsets, considered as a surrogate of the RR time interval. The MATLAB code for these preliminary analyses is open source and freely available at www.physionet.org.

2.3. Spectral analysis

For each beat-to-beat series (RR, SAP, DAP, PP), the mean value and the standard deviation were assessed. The series were then filtered with an adaptive filter (Wessel *et al* 2000) in order to remove artifacts and/or ectopic beats, and then detrended. Subsequently, they were resampled at 2 Hz. The spectral analysis was performed with an autoregressive model. Powers in very low frequency band (VLF, 0–0.04 Hz), low frequency band (LF, 0.04–0.15 Hz) and high frequency band (HF, 0.15–0.4 Hz) were computed, as well as the total power. The optimal model order was set to be in a range between 8 and 12.

The meaning of these frequency bands is similar to what has been reported for humans (Horner *et al* 1996, von Borell *et al* 2007). LF oscillations are associated with the sympathetic autonomic nervous system and HF oscillation with the ANS and respiratory mechanical effects.

2.4. Baroreflex analysis

2.4.1. Granger causality test. For each SAP and RR series a Granger causality test was performed in order to verify if the baroreflex control was still active under a compromised condition, such as after a CA. Briefly, a time series $u(n)$ is said to Granger-cause the series $y(n)$ if the knowledge of a certain number of past values of y and u are more helpful to predict y than the exclusive knowledge of past values of y (Söderström and Stoica 1988, Bassani *et al* 2012). Assuming that variables u and y are stochastic and stationary, we assessed the Granger causality by computing the F statistics, as reported in Bassani *et al* (2012) and Dorantes Mendez *et al* (2013).

Both feedback (FB) and feedforward (FF) pathways were tested by considering input SAP and RR series as exogenous, respectively. The causal relationship from SBP to RR (FB) represents the cardiac baroreflex, i.e. the actual FB mechanism, whereas the relationship from RR to SBP represents the direct influence of RR interval on SBP, which is not mediated by autonomic control, but instead by a perturbation mechanism based on the Starling law and diastolic runoff (Baselli *et al* 1988, Bassani *et al* 2012, Dorantes Mendez *et al* 2013).

The order of the models was set to be eight and we used a significance level of 0.05. The Granger test was performed for each experimental phase and both for feedback and feedforward mechanisms.

2.4.2. Baroreflex estimation: technical issues. The baroreflex sensitivity was estimated by adopting several well-known methods: the power ratio (Mortara *et al* 1997, Radaelli and Perlangeli 1999), the transfer function (Pinna and Maestri 2001) and the bivariate model (Bassani *et al* 2012, Dorantes Mendez *et al* 2013). All these methods rely on the computation of a coherence function $k^2(f)$. The coherence function estimates the degree of coupling between two signals in the frequency domain. Two signals are usually considered correlated when the coherence magnitude is greater than a fixed threshold 0.5. However, one important issue to address was the low variability in the cardiovascular signals and thus low values in the coherence function. As for CA, severe pathological conditions may dramatically affect the power in each individual signal so to end up with extremely low coherence values (Mortara *et al* 1997, Radaelli and Perlangeli 1999, Pinna and Maestri 2001). In this case, the choice of a fixed threshold could compromise the correct interpretation of the coherence function. In the literature, two different approaches were proposed to overcome this situation. Pinna and Maestri (2002) proposed not to apply any threshold in conditions of low signal-to-noise ratio and/or impaired baroreflex gain with a markedly reduced coherence. A second approach proposed by Faes *et al* (2004) consists in assessing a 'tailored' threshold for each frequency by computing an ensemble of N pairs of surrogate time series according to the surrogated method illustrated in Schreiber and Schmitz (2000). The coherence is then estimated between each pair of surrogate series and finally its empirical sampling distribution (frequency histogram) is calculated. The threshold function $T(f)$ used for the null hypothesis of no coherence is estimated as the 95th percentile of the coherence sampling distribution, to have a significance level of 0.05.

The power ratio method (α_{PR}) consists in computing the ratio between the SAP and RR spectra in the LF and HF band separately. The transfer function method consists in estimating the average gain of the transfer function (TF) from SAP to RR in LF and HF bands respectively. These methods were applied both without considering the coherence function and by assessing the power ratio and the average of transfer function only for those frequencies corresponding to a significant coherence, i.e. where $k^2(f) > T(f)$.

The bivariate model approach assesses BRS by considering the causal relationship from SBP to RR and RR to SBP (Barbieri *et al* 2002). Briefly, an autoregressive bivariate model of order $p = 8$ was computed as follows:

$$Y[n] = \sum_{k=1}^{p} A[k]\, Y[n-k] + W[n] \tag{1}$$

where

$$A[k] = \begin{bmatrix} a_{11}[k] & a_{12}[k] \\ a_{21}[k] & a_{22}[k] \end{bmatrix}, Y[n] = \begin{bmatrix} \mathrm{RR}[n] \\ \mathrm{SBP}[n] \end{bmatrix}, W[n] = \begin{bmatrix} W_{\mathrm{RR}}[n] \\ W_{\mathrm{SBP}}[n] \end{bmatrix} \tag{2}$$

and the coefficients a_{ij} were then used to calculate the gains of the transfer functions:

$$G_{\mathrm{SBP}\rightarrow\mathrm{RR}}(f)=\frac{A_{12}(f)}{1-A_{11}(f)} \qquad G_{\mathrm{RR}\rightarrow\mathrm{SBP}}(f)=\frac{A_{21}(f)}{1-A_{22}(f)} \tag{3}$$

where $A_{ij}(f)=\sum_{k=1}^{p} a_{ij}[k]\,\mathrm{e}^{-j2\pi fk}$.

As for the other methods, the values of the gains $G_{\mathrm{SBP}\rightarrow\mathrm{RR}}$ and $G_{\mathrm{RR}\rightarrow\mathrm{SBP}}$ were computed by averaging the gain values in the LF and HF band, respectively, and by averaging the gain values only for those frequencies associated to a significant coherence according to a threshold function.

2.4.3. Impulse response method. The cardiac baroreflex can also be investigated by considering a minimal closed loop model. RR fluctuations are assumed to depend on SBP fluctuations through arterial baroreflex (ABR) whereas SBP fluctuations reflect the Windkessel runoff effects (circulatory dynamics, CID) (Khoo 2008):

$$\Delta\mathrm{RR}(i)=\sum_{j=1}^{m} h_{\mathrm{ABR}}(j)\cdot \mathrm{SBP}(i-j-T_{\mathrm{ABR}})+w_{\mathrm{RRI}}(i) \tag{4}$$

$$\Delta\mathrm{SBP}(i)=\sum_{j=1}^{m} h_{\mathrm{CID}}(j)\cdot \mathrm{RRI}(i-j-T_{\mathrm{CID}})+w_{\mathrm{SBP}}(i) \tag{5}$$

where $h_{\mathrm{ABR}}(m)$ and $h_{\mathrm{CID}}(m)$ represent respectively the impulse response of the ABR or feedback mechanism and the impulse response of the CID or feedforward mechanism. By definition, the impulse response provides a complete characterization of the dynamics properties of the system, since the response of this system to any arbitrary input can be predicted by mathematically convolving the input with the impulse response (Khoo 2008). For instance, $h_{\mathrm{ABR}}(m)$ quantifies the time course of the change in RR series from an abrupt increase in SAP of 1 mmhg.

We estimated $h_{\mathrm{ABR}}(m)$ and $h_{\mathrm{CID}}(m)$ by using the Laguerre basis function according to Marmarelis (1993). Successively, the peak-to-peak amplitude and the peak-delay of impulse response $h_{\mathrm{ABR}}(m)$ were used in order to describe the magnitude and the rapidity of baroreflex regulation mechanism respectively.

2.5. Statistical analyses

Each index is represented as mean ± SD for each experimental phase. A one-way ANOVA for repeated measures was performed for each index, with experimental epochs being the repeated factor. Post hoc comparisons were performed using Student's paired *t*-test to compare the post-resuscitation epochs with the pre-CA epoch.

The values from argon and control groups were compared by an unpaired two-sample Student's test. A two tailed *p*-value less than 0.05 is considered statistically significant.

We considered parametric tests as we evaluated the symmetry of the sample distribution around median value by using boxplots.

3. Results

3.1. Time domain and spectral indices

After CA, the average values of RR and PP decreased without any recovery over time (table 1). In contrast, the SAP and DAP mean values diminished after CA and then tended to recover within 4 h after resuscitation. In particular, SAP and DAP mean values at Pr 3 h, Pr 4 h were

Table 1. The values of time domain and frequency domain indices are reported as mean ± SD for all the experimental phases. In the last column the *p*-values of the one-way ANOVA for repeated measure are reported.

	Pre-Ca	Pr 1 h	Pr 2 h	Pr 3 h	Pr 4 h	One way ANOVA
RR mean (ms)	621.9 ± 139.9	438.5 ± 108.4[a]	434.6 ± 75.0[a]	460.2 ± 101.8[a]	443.4 ± 76.0[a]	$p < 0.01$
RR SD (ms)	9.78 ± 7.42	4.52 ± 2.12[a]	6.01 ± 1.79	5.63 ± 2.54	6.06 ± 2.23	$p < 0.05$
SAP mean (mmHg)	118.6 ± 13.5	98.4 ± 12.9[a]	107.4 ± 12.1[a]	110.7 ± 14.0[b]	111.6 ± 13.2[b,c]	$p < 0.01$
DAP mean (mmHg)	95.12 ± 11.10	79.80 ± 14.31[a]	90.00 ± 13.43	93.15 ± 14.48[b]	93.74 ± 13.26[b,c]	$p < 0.01$
PP mean (mmHg)	23.48 ± 4.26	18.53 ± 3.22[a]	17.47 ± 3.61[a]	17.67 ± 4.02[a,b]	17.80 ± 3.54[a]	$p < 0.01$
RR LF (ms^2)	19.13 ± 36.37	1.76 ± 1.62	2.51 ± 2.85	4.26 ± 4.42	4.66 ± 4.28	n.s.
RR HF (ms^2)	16.40 ± 22.35	2.69 ± 2.02	3.43 ± 2.80[b]	5.75 ± 5.31[c]	5.93 ± 5.55[b,c]	$p < 0.05$
RR total power (ms^2)	44.73 ± 48.47	8.61 ± 6.15[a]	12.64 ± 7.99[a]	16.43 ± 12.75	16.94 ± 13.30[b,c]	$p < 0.01$
SAP LF ($mmHg^2$)	1.21 ± 2.12	0.50 ± 0.47	0.51 ± 0.48	1.27 ± 1.52	1.16 ± 2.10	n.s.
SAP HF ($mmHg^2$)	1.41 ± 1.89	2.05 ± 2.43	1.77 ± 0.95	1.94 ± 2.97	3.02 ± 5.25	n.s.
SAP total power ($mmHg^2$)	6.78 ± 6.36	4.49 ± 3.71	4.37 ± 2.11	6.07 ± 7.51	5.36 ± 5.61	n.s.
DAP LF ($mmHg^2$)	3.87 ± 6.91	0.48 ± 0.55	0.51 ± 0.43	0.98 ± 1.13	1.06 ± 2.08	n.s.
DAP HF ($mmHg^2$)	2.28 ± 2.50	3.12 ± 3.08	2.93 ± 1.90	3.39 ± 5.78	2.79 ± 3.04	n.s.
DAP total power ($mmHg^2$)	2.99 ± 2.65	3.04 ± 2.90	3.06 ± 1.24	4.97 ± 6.27	5.69 ± 6.67	n.s.

[a,b,c] Post hoc comparisons versus Pre-CA, Pr 1 h, Pr 2 h epoch, respectively.

significantly higher than the ones at Pr 1 h, Pr 2 h, as reported in table 1. The standard deviation of RR has a similar trend as well.

The absolute RR power in LF band showed a decreasing trend after CA, which tended to recover in the following resuscitation period, even though the values were not significant. The LF components of SAP and DAP showed a similar U-shape trend.

RR power in HF band changed significantly during the different experimental epochs: the values in pre-CA were significantly higher than the values at Pr 1 h, Pr 2 h, (table 1) and the values during the last two hours of the experiment were significantly higher with respect to the first two post-resuscitation epochs. However, the HF components of the other blood pressure variables did not show any significant change over time and they remained stable. We recall that HF components in SAP, DAP and PP do not represent any autonomic response, but only the mechanical effect of the respiratory activity.

RR total power diminished after the onset of the impairing condition and recovered in the following post-resuscitation epochs. The total power of SAP, DAP and PP did not show any particular pattern.

3.2. Baroreflex indices

In the majority of the epochs the pigs passed the Granger causality test. In particular, in Pre-CA, Pr 1 h, Pr 2 h, Pr 3 h, Pr 4 h the number of pigs that passed the test were 11, 11, 10, 9, 7 for the FF relationship, and 9, 11, 6, 6, 8 for the FB relationship, respectively.

Table 2 reports the values of the baroreflex sensitivity estimated with the different procedures. The values have different ranges according to the applied method; in particular the BRS values of the bivariate model have the lowest ones, as expected (Dorantes Mendez *et al* 2013). After CA the values of the baroreflex sensitivity dropped with a successive partial recovery in the post-resuscitation epochs. In fact, the values in the pre-CA epoch were significantly higher than values at Pr 1 h and Pr 2 h, as well as Pr 3 h and Pr 4 h values were significantly greater than values at Pr 1 h and Pr 2 h. As figure 1 shows, the values of the BRS gain show a trend with a U-shape suggesting a partial recovery of baroreflex.

Finally, the feedforward gain $G_{\mathrm{RR}\rightarrow\mathrm{SBP}}$ in the HF band was significant greater in Pr 1 h than in all other phases (table 2).

3.3. Impulse response analysis

The results from the impulse response analysis are reported in table 3. The magnitude of the ABR was significantly lower in the post resuscitation period with respect to pre-CA epoch, and it remained lower for all the post resuscitation period. Figure 2 shows the reduction of the average ABR peak delay through the different experimental epochs. The peak delay values were on average lower at the end of the experiment than the previous epochs, although not significantly.

3.4. Comparisons between argon and control groups

The results and trends obtained in the two groups were similar to the findings obtained by considering the pigs as a unique group. However, there were no significant differences between the two groups (figure 3).

Table 2. The values of the baroreflex indices are reported as mean ± SD for all the experimental phases. In the last column the *p*-values of the one-way ANOVA for repeated measure are reported.

		Pre-Ca	Pr 1 h	Pr 2 h	Pr 3 h	Pr 4 h	One way ANOVA
No thresholds on $k^2(f)$	α_{PR} LF ms mmHg^{-1}	4.13 ± 2.90	2.64 ± 2.09[a]	2.42 ± 1.61[a]	2.83 ± 1.75[c]	3.26 ± 2.12[c]	$p < 0.01$
	TF LF ms mmHg^{-1}	3.26 ± 2.04	1.74 ± 1.70[a]	1.42 ± 0.56[a]	2.01 ± 1.13[a,c]	2.20 ± 1.44[a,c]	$p < 0.01$
	$G_{SBP \rightarrow RR}$ LF ms mmHg	2.32 ± 2.26	0.71 ± 0.42[a]	0.71 ± 0.34[a]	1.14 ± 0.79[b,c]	0.98 ± 1.02	$p < 0.01$
	α_{PR} HF ms mmHg^{-1}	3.22 ± 3.50	1.34 ± 1.41	1.22 ± 0.83	1.91 ± 1.37	1.78 ± 1.22	n.s.
	TF HF ms mmHg^{-1}	3.57 ± 2.32	1.61 ± 1.25[a]	1.86 ± 0.60[a]	2.07 ± 1.09	2.13 ± 1.12	$p < 0.05$
	$G_{SBP \rightarrow RR}$ HF ms mmHg^{-1}	1.97 ± 1.03	1.05 ± 0.67	1.07 ± 0.43	1.26 ± 0.73	1.37 ± 1.34	$p < 0.01$
	$G_{RR \rightarrow SBP}$ LF mmHg ms^{-1}	0.19 ± 0.13	0.33 ± 0.31	0.20 ± 0.13	0.24 ± 0.22	0.23 ± 0.27	n.s.
	$G_{RR \rightarrow SBP}$ HF mmHg ms^{-1}	0.06 ± 0.04	0.11 ± 0.05[a]	0.06 ± 0.03[b]	0.08 ± 0.06[b]	0.07 ± 0.05[b]	$p < 0.05$
Thresholds on $k^2(f)$ estimated with the surrogate method	TF LF ms mmHg^{-1}	4.12 ± 3.29	1.95 ± 1.96[a]	1.75 ± 0.87[a]	2.26 ± 1.21[a,c]	2.50 ± 1.54[c]	$p < 0.01$
	TF HF ms mmHg^{-1}	3.48 ± 3.33	1.80 ± 1.51	2.06 ± 0.65	2.35 ± 1.31	2.41 ± 1.32	n.s.
	$G_{RR \rightarrow SBP}$ LF mmHg ms^{-1}	2.16 ± 1.97	0.53 ± 0.40	0.54 ± 0.22	1.19 ± 1.02	1.14 ± 1.14	n.s.
	$G_{SBP \rightarrow RR}$ HF ms mmHg^{-1}	1.88 ± 1.43	1.22 ± 0.90	1.36 ± 0.45	1.12 ± 0.27	2.03 ± 2.15	n.s.

[a,b,c] Post hoc comparisons versus Pre-CA, Pr 1 h, Pr 2 h epoch, respectively.

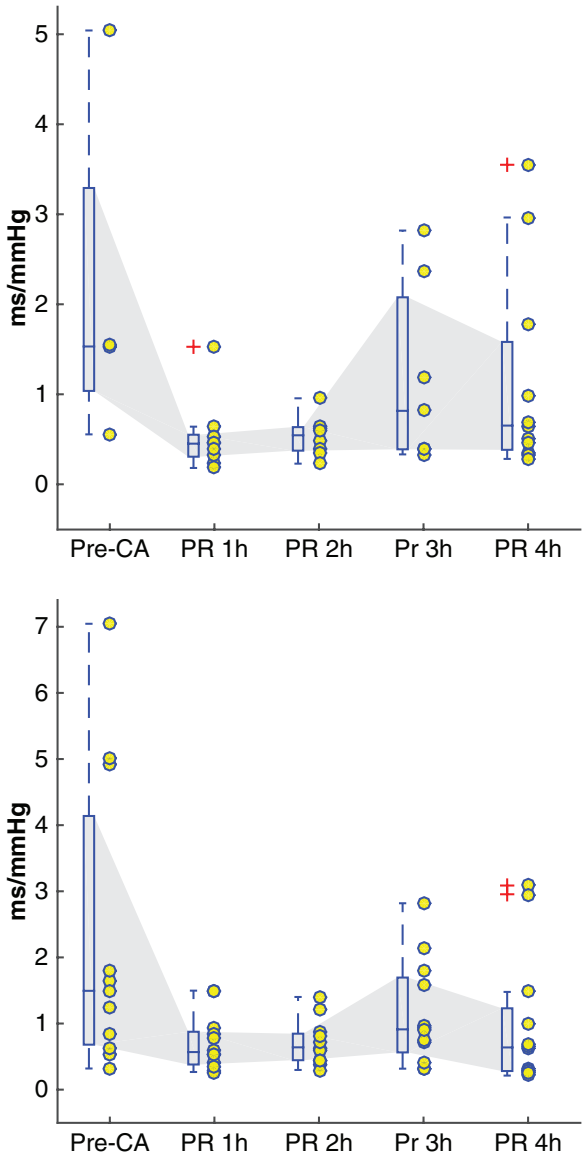

Figure 1. Boxplots of BRS gain values estimated with the bivariate model in LF band without applying a threshold on the cross-spectrum (upper panel) and by applying the surrogate method on the coherence function (lower panel). The grey region marks the 25° and 75° range interval. The circles mark the values of each single pig.

4. Discussion

In the time domain, both RR and pressure variable averages present significant changes during the experimental epochs. Furthermore, RR and PP do not recover after CA and their values are significantly lower with respect to the values measures before the event. In contrast, SAP and DAP increase with the time course of the experiment, i.e. after resuscitation. In the frequency domain, RR total power and the power in HF band diminish after the onset of the impairing

Table 3. The values of the impulse response parameters are reported as mean ± SD for all the experimental phases. In the last column the *p*-values of the one-way ANOVA for repeated measure are reported.

	Pre-Ca	Pr 1 h	Pr 2 h	Pr 3 h	Pr 4 h	One way ANOVA
ABR magnitude (ms mmHg^{-1})	2.77 ± 2.22	0.95 ± 0.69[a]	0.96 ± 0.53[a]	0.90 ± 0.73[a]	0.89 ± 0.52[a]	$p < 0.01$
Peak-to-peak delay (s)	0.80 ± 0.56	0.69 ± 0.28	8.75 ± 26.70	0.77 ± 0.43	0.58 ± 0.16	n.s.

[a] Post hoc comparisons versus Pre-CA, Pr 1 h, Pr 2 h epoch, respectively.

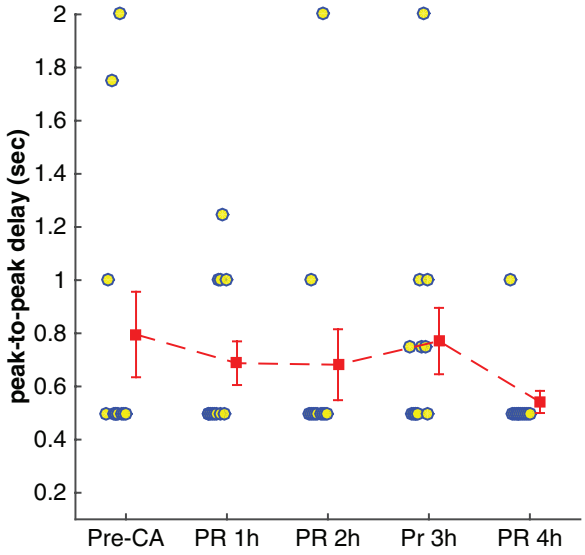

Figure 2. The values of $h_{ABR}(m)$ peak-to-peak delay are reported as mean ± SE in the different experimental epochs. The circles mark the values of each single pig.

condition and recover in the following post-resuscitation epochs. The results from the Granger causality test are in line with the hypothesis that the ANS control of the heart rate and circulation is still active. Although such control system is impaired the results of Granger causality test support the successive BRS analyses.

All of the estimators adopted in this study show a significant decrease of the baroreflex sensitivity after CA. However, partial recovery is obtained 3 or 4 h after resuscitation (figure 1).

Two possible explanations for this U-shape trend can be elicited from our results. The first one is the electrical instability of the organ effector, as in the closed loop system the regulation of ABP through CO is mediated by the heart functioning. This hypothesis would also explain the decrease in the RR interval values, the trend of $G_{RR \rightarrow SBP}$ values in the post-resuscitation epochs and the reduced values of partial coherence $k^2(f)_{RR \rightarrow SBP}$.

A second hypothesis is related to a possible decline in the vagal control. Even though the mechanical ventilation influences the HF oscillations of the RR series, table 1 shows a recovery of the HF component after a drop following CA. The reduction of vagal stimulation and its recovery are supposed to drive the BRS recovery. The impulse response analyses allowed investigating the baroreflex not only in terms of gain, but also in terms of temporal dynamics. The ABR

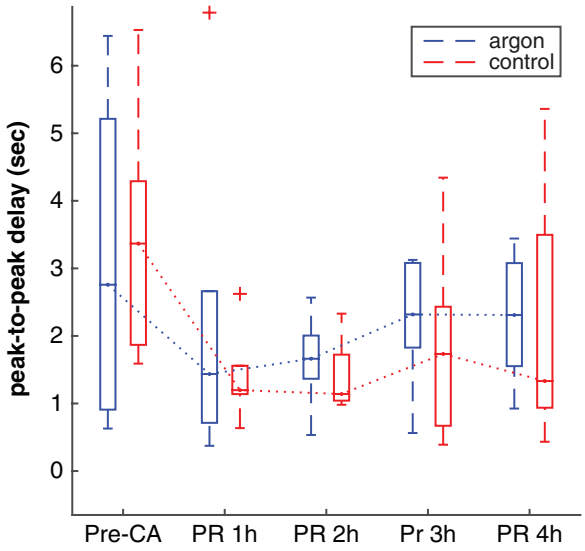

Figure 3. Boxplots of BRS values in LF band, estimated with the transfer function during each experimental epoch in the two different groups of animals.

delay reduced after CA and was significantly shorter at Pr 4 h. This finding hints a compensation mechanism: a faster response when baroreflex gain is not fully restored. The increase in the speed of baroreflex response is in line with the hyphothesis of a key role of the parasympathetic nervous system (PSNS), which is known to act at a higher firing rate (Cerati and Schwartz 1991).

Furthermore, a depression of PSNS control represents a reduction of protection from cardiac arrhythmia, such as ventricular fibrillation, as described in Babai *et al* (2002).

There is growing literature to support the importance of preserving ANS after CA and other severe hypoxic-ischemic insults. Thus, loss of ANS has been associated with increased mortality not only after AMI, but also after brain injury, sepsis with multiple organ dysfunction, trauma and CA. Moreover, the degree of ANS depression has been associated with the extent of cell death and inflammation, also in the brain and not only specifically in the heart (Norman *et al* 2012). Indeed, earlier experimental and clinical studies on CA have reported a decreased activity of ANS after CA and more specifically in the instance of poor outcome (Chen *et al* 2009, Li *et al* 2012). CA, in fact, is a whole body ischemia reperfusion event and the main target organ, together with the heart, is represented by the brain. Severe brain damage and neurological dysfunction are indeed the major cause of death. The ischemic insult to the brain may therefore alter the cardiac vagal motor neurons centrally, located in the medulla in the dorsal motor nucleus and the nucleus ambiguous (Travagli and Gillis 1994). The post-resuscitation period is marked by hemodynamic instability and is related to the release of many inflammatory cytokines, with activation of systemic inflammation and stress hormones after return of spontaneous circulation (ROSC) (Ristagno *et al* 2015), which may be another mechanism affecting directly cardiac autonomic nervous dysfunction. When a well-established protective intervention was performed, a better post-resuscitation heart rate variability (HRV) was observed, consistent with higher rate of favorable outcome, i.e. both survival and neurological recovery.

In conclusion, we confirmed in the present study the transient reduction in ANS control after CA and we hypothesize the PSNS as a key role in preventing secondary effects to CA. Nevertheless, all earlier studies investigating the relationship between CA, ANS and outcome, evaluated ANS by assessing HRV only. In contrast to HRV alone, our approach however

presents the advantage of assessing the BRS, which is the direct expression of nervous regulation on the heart rate and arterial blood.

4.1. Limitations

The main limitation of the present work is represented by the available observational period after resuscitation, in further studies a much longer time period should be beneficial, for example 12 h as proposed in De Ferrari *et al* (2014). Another limit could be the use of heart period instead of the RR intervals estimated directly in the ECG traces. This choice was compelled by the fact that the ECG traces showed an ST elevation, accompanied by a large T wave whose extent is comparable with R peak. The automatic classification algorithm frequently confounded the T wave with an R peak, introducing a fake variability in RR series.

5. Conclusion

The present study investigates the BRS by means of different methods for each experimental epoch after CA and our results confirm the presence of a partial recovery in the post-resuscitation period. However, argon has no role in the baroreflex changes after CA and, in general, the autonomous nervous system functions. Finally, spectral analyses and impulse response investigations draw attention to some control mechanisms, which may play a role after CA. In conclusion, we hypothesize that a recovery of the vagal stimulation elicited by a faster dynamics in the baroreflex could drive baroreflex recovery.

Acknowledgments

This research is supported by the EU FP7 Health Programme, ShockOmics project, Grant #602706.

References

Aletti F, Ferrario M, Xu D, Greaves D K, Shoemaker J K, Arbeille P, Baselli G and Hughson R L 2012 Short-term variability of blood pressure: effects of lower-body negative pressure and long-duration bed rest *Am. J. Physiol. Regul. Integr. Comp. Physiol.* **303** R77–85

Babai L, Papp J G, Parratt J R and Vegh A 2002 The antiarrhythmic effects of ischaemic preconditioning in anaesthetized dogs are prevented by atropine; role of changes in baroreceptor reflex sensitivity *Br. J. Pharmacol.* **135** 55–64

Barbieri R, Parati G and Saul J P 2001 Closed- versus open-loop assessment of heart rate baroreflex *IEEE Eng. Med. Biol. Mag.* **20** 33–42

Barbieri R, Triedman J K, Saul J P 2002 Heart rate control and mechanical cardiopulmonary coupling to assess central volume: a systems analysis *Am. J. Physiol. Regul. Integr. Comp. Physiol.* **283** R1210–20

Baselli G, Cerutti S, Civardi S, Malliani A and Pagani M 1988 Cardiovascular variability signals: towards the identification of a closed-loop model of the neural control mechanisms. *IEEE Trans. Biomed. Eng.* **35** 1033–46

Bassani T, Magagnin V, Guzzetti S, Baselli G, Citerio G and Porta A 2012 Testing the involvement of baroreflex during general anesthesia through Granger causality approach *Comput. Biol. Med.* **42** 306–12

Cerati D and Schwartz P J 1991 Single cardiac vagal fiber activity, acute myocardial ischemia, and risk for sudden death *Circ. Res.* **69** 1389–401

Chen W L, Tsai T H, Huang C C, Chen J H and Kuo C D 2009 Heart rate variability predicts short-term outcome for successfully resuscitated patients with out-of-hospital cardiac arrest *Resuscitation* **80** 1114–8

De Ferrari G M *et al* 2014 Rapid recovery of baroreceptor reflexes in acute myocardial infarction is a marker of effective tissue reperfusion *J. Cardiovasc. Transl. Res.* 553–9
Dorantes Mendez G, Aletti F, Toschi N, Canichella A, Dauri M, Coniglione F, Guerrisi M, Signorini M G, Cerutti S and Ferrario M 2013 Baroreflex sensitivity variations in response to propofol anesthesia: comparison between normotensive and hypertensive patients *J. Clin. Monit. Comput.* **27** 417–26
Faes L, Pinna G D, Porta A, Maestri R and Nollo G 2004 Surrogate data analysis for assessing the significance of the coherence function *IEEE Trans. Biomed. Eng.* **51** 1156–66
Gräsner J-T and Bossaert L 2013 Epidemiology and management of cardiac arrest: what registries are revealing. *Best Pract. Res. Clin. Anaesthesiol.* **27** 293–306
Horner S M *et al* 1996 Contribution to heart rate variability by mechanoelectric feedback. Stretch of the sinoatrial node reduces heart rate variability *Circulation* **94** 1762–7
Khoo M C K 2008 Modeling of autonomic control in sleep-disordered breathing *Cardiovasc. Eng.* **8** 30–41
La Rovere M T, Maestri R, Robbi E, Caporotondi A, Guazzotti G, Febo O and Pinna G D 2011 Comparison of the prognostic values of invasive and noninvasive assessments of baroreflex sensitivity in heart failure *J. Hypertens.* **29** 1546–52
Li Y, Ristagno G, Guan J, Barbut D, Bisera J, Weil M H and Tang W 2012 Preserved heart rate variability during therapeutic hypothermia correlated to 96 h neurological outcomes and survival in a pig model of cardiac arrest *Crit. Care Med.* **40** 580–6
Marmarelis V Z 1993 Identification of nonlinear biological systems using Laguerre expansions of kernels *Ann. Biomed. Eng.* **21** 573–89
Mortara A, La Rovere M T and Pinna G D *et al* 1997 Depressed arterial baroreflex sensitivity and not reduced heart rate variability identifies patients with chronic heart failure and nonsustained ventricular tachycardia: the effect of high ventricular filling pressure *Am. Heart J.* **134** 879–88
Nolan J P *et al* 2008 Post-cardiac arrest syndrome: epidemiology, pathophysiology, treatment, and prognostication: a scientific statement from the International Liaison Committee on Resuscitation; the American Heart Association Emergency Cardiovascular Care Committee; the Council on Cardiovascular Surgery and Anesthesia; the Council on Cardiopulmonary, Perioperative, and Critical Care; the Council on Clinical Cardiology; the Council on Stroke *Resuscitation* **79** 350–79
Norman G J, Karelina K, Berntson G G, Morris J S, Zhang N and Devries A C 2012 Heart rate variability predicts cell death and inflammatory responses to global cerebral ischemia *Front. Physiol.* **3** 131
Pinna G and Maestri R 2001 Reliability of transfer function estimates in cardiovascular variability analysis *Med. Biol. Eng. Comput.* **39** 338–47
Pinna G D and Maestri R 2002 New criteria for estimating baroreflex sensitivity using the transfer function method *Med. Biol. Eng. Comput.* **40** 79–84
Podrid P J and Myerburg R J 2005 Epidemiology and stratification of risk for sudden cardiac death *Clin. Cardiol.* **28** I3–11
Porta A, Baselli G, Cerutti S 2006 Implicit and explicit model-based signal processing for the analysis of short-term cardiovascular interactions. *Proc. IEEE* **94** 805–18
Radaelli A and Perlangeli S 1999 Altered blood pressure variability in patients with congestive heart failure *J. Hypertens.* **17** 1905–10
Ristagno G *et al* 2014 Postresuscitation treatment with argon improves early neurological recovery in a porcine model of cardiac arrest *Shock* **41** 72–8
Ristagno G *et al* 2015 Copeptin levels are associated with organ dysfunction and death in the intensive care unit after out-of-hospital cardiac arrest *Crit. Care* **19** 132
Ristagno G, Tang W, Xu T Y, Sun S and Weil M H 2007 Outcomes of CPR in the presence of partial occlusion of left anterior descending coronary artery *Resuscitation* **75** 357–65
Schreiber T and Schmitz A 2000 Surrogate time series *Physica* D **142** 346–82
Söderström T and Stoica P 1988 *System Identification* (Englewood Cliffs, NJ: Prentice-Hall)
Travagli R A and Gillis R A 1994 Nitric oxide-mediated excitatory effect on neurons of dorsal motor nucleus of vagus *Am. J. Physiol. Gastrointest. Liver Physiol.* **266** G154–60
von Borell E *et al* 2007 Heart rate variability as a measure of autonomic regulation of cardiac activity for assessing stress and welfare in farm animals—a review *Physiol. Behav.* **92** 293–316
Wessel N *et al* 2000 Nonlinear analysis of complex phenomena in cardiological data *Herzschrittmachertherapie Elektrophysiologie* **11** 159–73
Zong W, Heldt T, Moody G B and Mark R G 2003 An open-source algorithm to detect onset of arterial blood pressure pulses *Comput. Cardiol.* **30** 259–62